Frequency Analysis of a Redox-Based Molecular-Electrical Communication Channel

Karthik Reddy Gorla
School of Computing, University of Nebraska-Lincoln
Lincoln, Nebraska, USA
karthikr.gorla@huskers.unl.edu

Massimiliano Pierobon
School of Computing, University of Nebraska-Lincoln
Lincoln, Nebraska, USA
maxp@unl.edu

ABSTRACT

The realization of interfaces between the biological world and electronics has the potential to propel the field of Molecular Communication (MC) to novel frontiers. Plugging MC-enabled devices to our electrical cyber-world will enable revolutionary applications, especially in the biomedical field. By stemming from a seminal proof-of-concept prototype that enables communication between a biological system and an electrical circuit, based on redox biochemical reactions, this paper introduces the first frequency analysis of such system and its characterization in terms of communication performance (capacity). To achieve these results, made possible by a linearity property in the analytical model of the system, an empirical methodology is followed to obtain the frequency response and the noise power spectral density of the system from the results of a simulation framework. The latter was developed in prior work and made accessible publicly through a web app. A water filling capacity estimation algorithm is applied to the obtained results to give a preliminary idea on the communication performance of such system, which results in a transmission rate equivalent to 0.0587 bits/hour. While orders of magnitude slower than common electrical or optical communications, these results are in line with the inherent timescales of the biological systems envisioned to be interfaced with this technology.

CCS CONCEPTS

• **Mathematics of computing** → **Information theory**; • **Computing methodologies** → **Modeling and simulation**.

KEYWORDS

Molecular communication; Redox channel; Diffusion noise; Cyclic voltammetry; Frequency Analysis; Power Spectral Density; Water filling Algorithm

ACM Reference Format:
Karthik Reddy Gorla and Massimiliano Pierobon. 2023. Frequency Analysis of a Redox-Based Molecular-Electrical Communication Channel. In *10th ACM International Conference on Nanoscale Computing and Communication (NANOCOM '23), September 20–22, 2023, Coventry, United Kingdom.* ACM, New York, NY, USA, 6 pages. https://doi.org/10.1145/3576781.3608724

NANOCOM '23, September 20–22, 2023, Coventry, United Kingdom

ACM ISBN 979-8-4007-0034-7/23/09…$15.00
https://doi.org/10.1145/3576781.3608724

1 INTRODUCTION

Molecular Communication (MC) has emerged as a promising field, enabling new possibilities in the development of devices and systems at the biomolecular and nanoscale domains [1]. Research in MC leverages the intrinsic properties of molecules to transmit information, and the natural systems already exploiting them, paving the way for innovative applications in areas such as targeted drug delivery, biosensing, and nanoscale robotics [2]. However, one of the main hurdles for MC to become a viable technology is the realization of reliable interfaces between the biomolecular world and the electronic domain [3]. These interfaces are crucial for the effective translation of signals between biological systems and electronic devices, ensuring seamless integration and performance. Overcoming this challenge is essential to unlock the full potential of MC and facilitate its widespread adoption in various applications.

In recent years, several works targeted the design and even the prototyping [4] of interfaces between MC and electronics, but few focused on interfacing specifically with the biological world. In this specific direction, a series of seminal works [5–7] was one of the first attempts to demonstrate experimentally that biochemical reactions called redox, where molecular species exchange electrons, can effectively propagate molecular information from a biological system to an electrical circuit (and *vice versa*). While an experimental proof-of-concept of this system was realized, its thorough performance characterization and modeling to support an engineering design process and optimization is currently missing. This investigation direction has the potential to result into engineering design rules and concepts and turn this first experimental proof into a viable architecture for future MC-enabled devices [3].

Research in the MC field has been instrumental in realizing tools to model, characterize, and control biochemical and nanoscale systems starting from the characterization of their communication performance metrics [8]. One of the challenges in the characterization of communication performance in MC systems that include biological component stems from the highly non-linear and complex nature of the corresponding mathematical models. The adopted approach has been to produce datasets through computational modeling/simulation or experimental activities, and then applying empirical tools to quantify communication performance and define potential design rules [9, 10].

In this paper, we propose an analysis and characterization of the aforementioned redox-based MC system in the frequency domain. In particular, we estimate the input-output transfer function of the system and the power spectral density of the noise resulting upon translation from the molecular to the electrical domain. These results are obtained through an empirical approach supported by a computational model and a simulation framework based in part on

our previous work [11]. For the first time, our frequency domain analysis enables the estimation of the theoretical system capacity, or achievable information rate, through an application of the water filling algorithm [12].

The rest of the paper is organized as follows. In Sec. 2, we detail the main concepts and mathematical formulas at the basis of the redox-based molecular-to-electrical system model, and their properties. The methodologies adopted for frequency analysis and water-filling capacity estimation are described in Sec. 3. Sec. 4 includes numerical results of the simulation model in terms of input-output frequency response, noise power spectral density, and the estimation of the channel capacity. Finally, we conclude the paper in Sec. 5.

2 SYSTEM MODEL

In this section, we briefly describe the main mathematical model components of the redox-based communication system considered in this paper and their implementation in the simulation framework. For more details on the system and its components, refer to [11]. This model is an abstraction of the experimental device described in [6]. Compared to the system model from [11], for this paper, we considered only the diffusion noise and not the reaction noise. A motivation for this choice is provided in Sec. 2.1.3.

The system model of the redox-based molecular-to-electrical communication is envisioned in Fig. 1, with the input signal from the **Source** being transmitted by the **Molecular Transmitter** as a change in concentration (concentration rate) of redox-active molecules (which can undergo redox reactions through the exchange of electrons) modulated through a given surface, propagating through the space via **Molecule Diffusion** before they reach the receiving electrode. **Diffusion Noise** due to Brownian motion affects this communication system. Upon reaching the receiving electrode, the redox-active molecules undergo **Redox Reactions** as function of the voltage at the electrode, resulting in an exchange of electrons that is measured as an electrical current, which is the output signal received at the **Electrical Receiver**, and sent to the **Destination**. In this system, information flows from a molecular domain to an electrical domain, namely, from an input concentration rate of molecules into an output electrical current, covering the distance from the transmitter (*e.g.*, biological cell culture) to the receiver (electrode) via diffusion.

2.1 System Model Components

2.1.1 Molecular Transmitter. The molecular transmitter as seen in Fig. 1 is abstracted as an ideal emitter that modulates the incoming redox-active molecules through a **Surface**, here for simplicity depicted as a disc. The redox-active molecules can be categorized into two states, namely oxidized and reduced. The oxidized state refers to the molecule chemical ionic state after losing one or more electrons, while the reduced state refers to the same after gaining one or more electrons [13]. The output from the transmitter $\mathrm{Tx}(t)$ can be expressed in terms of concentration rate, having the dimensions of moles per unit volume per unit time as

$$\mathrm{Tx}(t) = \frac{\partial}{\partial t}\begin{bmatrix} C_{1,O}(t) & .. & C_{m,O}(t) & .. & C_{M,O}(t) \\ C_{1,R}(t) & .. & C_{m,R}(t) & .. & C_{M,R}(t) \end{bmatrix}, \quad (1)$$

where $C_{m,S}(t)$ is the concentration of redox-active molecules of species m in redox state S (oxidized O or reduced R) at time t on the **Surface**. M is the total number of redox-active molecular species considered in the system ($M = 1$ for the results presented in Sec. 4).

2.1.2 Molecule Diffusion. The redox-active molecules emitted through the surface diffuse between the **Surface** and the **Electrode** through a liquid solution (called buffer solution or redox capacitor) [6]. This diffusion process is abstracted using the second Fick's law with inhomogeneous components [8]. The latter are due to the flux of incoming molecules through the surface and the change in redox state of the molecules reaching the electrode, respectively. This diffusion process is mathematically expressed as

$$\left\{ \frac{\partial C_{m,S}(x,t)}{\partial t} = D_m \nabla^2 C_{m,S}(x,t) \cdots \right. \\ \left. \cdots \pm \frac{I_m(t)}{n_m F A r} \delta(x-H) \right\}_{m=1,2,\ldots,M;S=O,R}, \quad (2)$$

where $C_{m,S}(x,t)$ is the concentration of redox-active molecules of species m in a redox state S (O or R) at time t and distance x, D_m is the diffusion coefficient of species m in the buffer solution, $I_m(t)$ is the current measured at the **Electrode** at time t, n_m is the number of electrons transferred per redox reaction, F is the Faraday constant [13], Ar is the cross-sectional area of the reacting surface of the **Electrode**. This equation has a boundary condition on the **Surface** expressed as

$$C_{m,S}(0,t) = C_{m,S}(t), \quad (3)$$

where $C_{m,S}(0,t)$ is the concentration of molecules of species m and redox state S at time t on the **Surface**, and $C_{m,S}(0,t)$ is the concentration of molecules of species m and redox state S at time t as part of the transmitter output $\mathrm{Tx}(t)$ expressed in (1).

As the molecules diffuse between the surface and the electrode, they are affected by diffusion noise caused by the discrete nature of molecules as well as the randomness in their movement attributed to Brownian motion. This diffusion noise can be modeled as a volumetric Poisson counting process [8] at the electrode with an expected rate equal to the concentration of redox-active molecules at the electrode. As a consequence, the resulting noisy concentration $C'(H,t)$ at the electrode is expressed as

$$C'(H,t) = \frac{N'(t)}{\Delta x A r \mathrm{N_A}}, \quad (4)$$

where $N'(t)$ is the actual number of molecules at time t as a result of the volumetric Poisson counting process with an expected rate equal to the concentration of a redox-active molecule in a finite space volume of size $\Delta x Ar$ at the **Electrode** (with a surface area of Ar and depth Δx [1], and $\mathrm{N_A}$ is the Avogadro's number.

2.1.3 Redox Reactions. Upon reaching the electrode, the redox-active molecules undergo redox reactions, *i.e.*, reduction or oxidation, as follows:

$$\mathrm{O} + \mathrm{ne} \underset{k_b}{\overset{k_f}{\rightleftharpoons}} \mathrm{R}, \quad (5)$$

[1] Δx is a finite perpendicular distance from the **Electrode**. It is also the maximum distance permissible in forming the finite space volume $\Delta x Ar$ without producing alias in the current output considering the input signal bandwidth (Table 3).

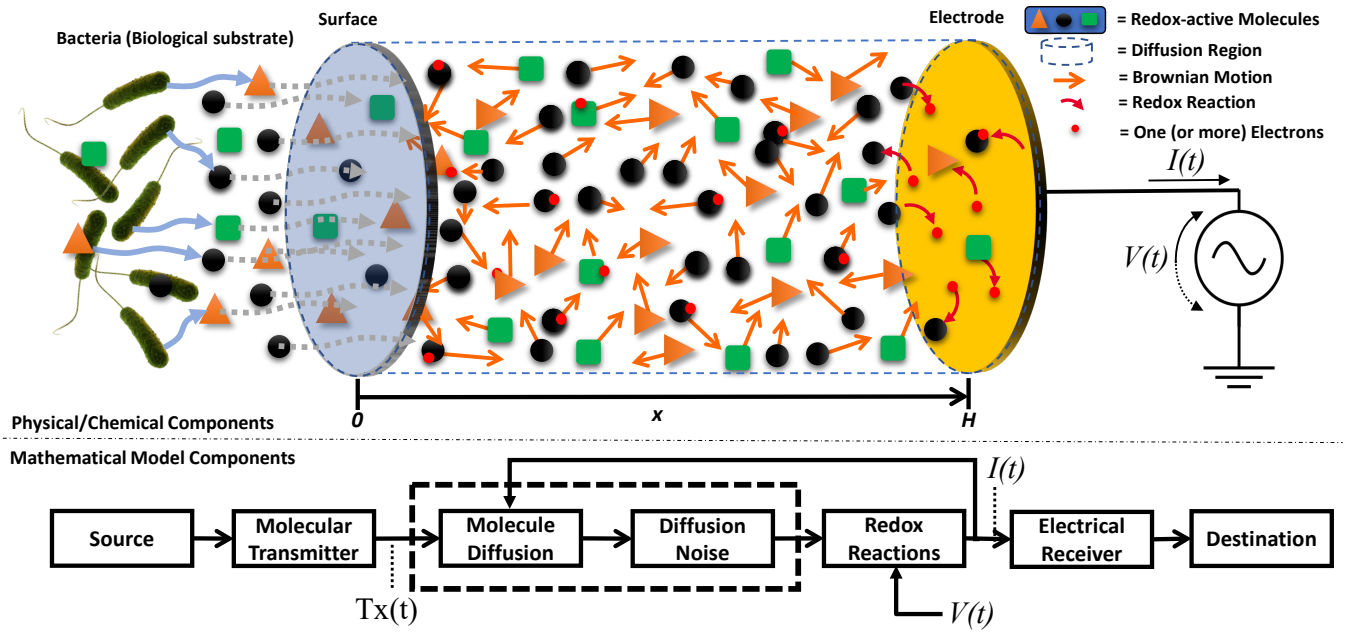

Figure 1: System components of the redox-based molecular-to-electrical communication.

where O and R are the the oxidized and the reduced states of the redox-active species, respectively, e is an electron, n is the number of electrons transferred, k_f and k_b are the forward and reverse reaction rate constants[2], respectively. The reaction rate constants of the redox reaction in (5) can be expressed as

$$k_{f_m}(t) = k_{0_m} e^{\frac{-\alpha_m n_m F}{RT}(V(t)-E^0_m)}, \tag{6}$$

$$k_{b_m}(t) = k_{0_m} e^{\frac{(1-\alpha_m) n_m F}{RT}(V(t)-E^0_m)}, \tag{7}$$

where k_{0_m} is the standard rate constant of species m, α_m is the charge transfer coefficient of species m, n_m is the number of electrons transferred per reaction of species m, F is the Faraday constant, R is the molar gas constant, T is the absolute temperature, $V(t)$ is the probing voltage applied at time t at the **Electrode**, and E^0_m is the standard potential of the redox-active molecule of species m undergoing the reaction [13][14].

In [11] the reaction noise was modeled based on the Stochastic Simulation Algorithm (SSA). This results in a noise that approximates to a temporal Poisson counting process [15]. In the scope of this paper, with the simulation setting and parameters used, the magnitude of the reaction noise was observed to be much lower than the magnitude of the diffusion noise, and therefore negligible in the current analysis. The impact and comparison of the two noises in other settings will be investigated in future work.

2.1.4 Electrical Receiver. The receiver is an electrode that acts as the gateway connecting the molecular to the electrical domain. The probing voltage signal $V(t)$, an auxiliary input to the system which governs the reaction rate of the redox reactions as in (6) and (7), is applied to the electrode as function of the time t through an external circuit. This voltage signal is a triangular wave as function of the time, expressed as

$$V(t) = \frac{2v_{Amp}}{\pi} \sin^{-1}(\sin(2\pi f t)), \tag{8}$$

where v_{Amp} is the maximum net amplitude of the voltage signal, and f is the frequency of the triangular wave. The use of a triangular voltage wave to probe redox-active species comes from a standard electrochemical analysis procedure called cyclic voltammetry (CV) [13], whose output is an electrical current dependent on the redox reactions occurring at the electrode, expressed as

$$I(t) = \sum_{m=1}^{M} n_m F A r [k_{f_m}(t) C'_{m,O}(H,t) \cdots \\ \cdots - k_{b_m}(t) C'_{m,R}(H,t)], \tag{9}$$

where $I(t)$ is the total measured output current at time t, $C'_{m,O}(H,t)$ and $C'_{m,R}(H,t)$ are the noisy concentration of species m in oxidized and reduced states as calculated from (4), respectively, at time t at the **Electrode**, n_m is the number of electrons transferred per reaction of species m, F is the Faraday constant, Ar is the cross-sectional area of the reacting surface of the **Electrode**, and k_{f_m}(t) and k_{b_m}(t) are the forward and backward reaction rate constants of species m at time t, respectively. The output of the system is defined as the absolute peak current (positive or negative) occurring in the generated electrical current signal. The peak current corresponds to the state when the output current saturates, and it is a common output parameter in CV [13].

[2] k_f and k_b are called reaction rate constants or reaction rate coefficients as per chemical kinetics terminology even if they are here defined as functions of time. This is because in this system they depend on a time-varying probing voltage, as expressed in (6) and (7).

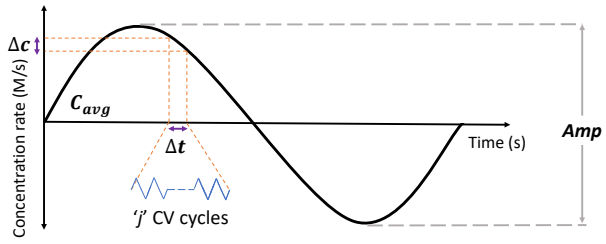

Figure 2: Input sinusoidal signal

2.2 Linearity

The redox-based molecular-electrical communication system detailed in Sec. 2.1 is characterized by a molecular input, an electrical current output and an auxiliary input probing voltage. While the auxiliary input probing voltage and the electrical current output have a nonlinear relationship, as per (6), (7), and (9), the relation between concentration of redox-active molecules at the electrode and the electrical current output is linear, as per (9). Given a specific redox-active species and an auxiliary voltage signal, the output electrical current is proportional to the redox-active molecule concentration at the electrode, which in turn is proportional to the input concentration rate according to the Fick's laws of diffusion. Therefore, the electrical current output signal (and its peaks) is proportional to the molecular concentration rate input signal.

Another theoretical proof of input-output linearity for this system stems from the Randles-Sevchik equation, which computes the peak current achieved as a function of the molecular concentration at the electrode, diffusion coefficient, scan rate, and other constants [16].

3 COMMUNICATION PERFORMANCE ANALYSIS TOOLS AND METRICS

The input-output linearity of the system model, as explained in Sec. 2.2, allows the application of linear system theory and tools, which greatly simplify the calculation of communication performance metrics through frequency domain analysis. Since the equations governing the system model detailed in Sec. 2.1 cannot be readily formulated into an input-output closed-form analytical expression, in this paper we follow an empirical methodology to obtain an estimation of the communication performance of the redox-based molecular-to-electrical communication channel. This methodology is based on the water filling algorithm [17] applied to a computational model of the system components described in Sec. 2. We developed the computational model using finite difference methods applied to CV simulation [18], and we implemented it into a simulation framework that we published as a freely available web application [19].

3.1 Empirical Frequency Analysis

In this paper, we are interested in calculating the frequency response of the redox-based molecular-to-electrical communication system, as well as the power spectral density of the resulting noise at the output of the system. The latter is then utilized for estimating the water-filling capacity of the system. With reference to the system model in Sec. 2, in the scope of this paper the frequency analysis is made for a **single redox-active molecule species**, *i.e.*, $M = 1$, and considering an input signal composed of molecules in only one of the two states S (reduced or oxidized), which results in the following transmitter output:

$$\mathrm{Tx}(t) = C_S(0,t)\,. \tag{10}$$

In this paper, we apply a set of sinusoidal input signals (with varying frequencies) to the system, and we record the corresponding simulated output signals. With reference to Fig. 2, each input signal to the simulation is a sinusoidal redox-active molecule concentration rate signal with a specific amplitude Amp around an average value c_{avg}, sampled with an interval Δt, expressed as

$$C_S(0, l\Delta t) = c_{avg} + Amp \sin\left(2\pi \frac{1}{\tau j L} l\Delta t\right), \tag{11}$$

where τ is the period in seconds of one CV triangular wave, as explained in Sec. 2.1.4, j is the number of CV cycles (number of triangular wave periods) that are performed within each sample interval Δt, l refers to the l^{th} sample of the input, and L is the total number of input samples to complete one period of the sinusoidal signal.

The bandwidth of the system being explored with the input signal in (11) is limited by the period τ of the CV probing voltage signal. In fact, this period is chosen as to obtain a stable CV output given the specific redox-active species considered in the system [13]. Once τ is set, the limit for obtaining an output response of the system in terms of peak of the output current $I(t)$, expressed in (9), is to sample the input signal with a minimum interval Δt corresponding to exactly one CV cycle. This minimum constraint on the sampling interval limits the maximum frequency that can be possibly applied to the input, according to the Nyquist-Shannon sampling theorem, to $\frac{1}{2\tau}$. Within the scope of this paper, once a specific redox-active molecule is considered, this limit defines the maximum operating bandwidth of the redox-based communication system. In our empirical frequency analysis, the frequency of the input signal (11) is selected by varying the number j of CV cycles per sample from a minimum of 1 to a maximum value, corresponding to the lowest probed frequency.

For each signal (11) applied to the computational model simulation of the system, we obtain an output current, whose peak value (positive or negative, depending on the specific redox-active species in the system) is considered the output at each sampling interval Δt. These output signal samples contain the linear response of the system to the input sinusoidal signal together with the contribution of the noise detailed in Sec. 2.1.2. The amplitude of the **frequency response of the channel** is obtained by extracting the amplitude of the main frequency component from the output signal (at a frequency equal to the frequency of the corresponding input signal) for each probed frequency, and by dividing it by the amplitude Amp of the input. The **noise power spectral density** $\mathrm{PSD}_{noise}\left(\frac{1}{\tau j L}\right)$ is instead obtained by dividing each sample of the output signal by the corresponding sample of the input signal, and then by computing the variance of the resulting values across all samples. We are aware that the calculation of the noise power spectral density is suboptimal given the Poissonian nature of the noise, but we believe

Table 1: Input Signal Parameters

Parameter	Value
Number of Samples (L)	100
Average Concentration (C_{avg})	$500fM$
Amplitude (Amp)	$200fM$
Time Period of one CV cycle (τ)	20 s
Frequency $\frac{1}{\tau jL}$ Range	$\left[\, 5\times10^{-6}, 5\times10^{-4} \,\right]$ Hz
Distinct Frequencies (J)	100

this can be useful for a preliminary investigation of the capacity, inspired by the work in [12].

3.2 Capacity Estimation through Water Filling

The water filling algorithm is applied to estimate the capacity of a channel affected by Gaussian additive noise with an optimal signal power allocation [17]. In the scope of this paper, although the noise is neither additive nor Gaussian, as detailed in Sec. 2.1.2, we apply this algorithm by following a similar methodology as described in [12], with the goal to provide an initial estimate of the redox-based communication channel capacity.

Our methodology comprises the following steps:

(1) Find the noise power spectral density as described in Sec. 3.1.
(2) Find the average power of the output signal, which corresponds to the desired average input power for which we set to estimate the water filling capacity. Let it be denoted as ν.
(3) Using the obtained average power as the "water line", find the power of the output signal without noise, which is the difference between the average power and the noise power at each frequency.
(4) Estimate the capacity through water filling by applying the Shannon-Hartley theorem [17] with the following expression:

$$C = \sum_{j=2}^{J} \left(\frac{1}{\tau(j-1)L} - \frac{1}{\tau jL} \right) \log_2 \left(1 + \frac{\nu - \mathrm{PSD}_{noise}\left(\frac{1}{\tau jL}\right)}{\mathrm{PSD}_{noise}\left(\frac{1}{\tau jL}\right)} \right), \quad (12)$$

where C is the capacity, ν is the desired average input power, $\mathrm{PSD}_{noise}\left(\frac{1}{\tau jL}\right)$ is the power spectral density of the noise at frequency $\frac{1}{\tau jL}$, and J is the total number of distinct frequencies used in the generation of input concentration signals across the range mentioned in Tab. 1.

4 NUMERICAL RESULTS

The parameters for the input signal (11) used in this paper to obtain the numerical results are detailed in Tab. 1. The frequency range corresponds to having from 100 down to 1 CV cycle(s) between two consecutive samples of the input signal in (11).

Ferrocene (Fc), a commonly used redox-active species, was chosen for the simulations [13][20]. The species-specific parameters are displayed in Tab. 2, and were estimated based on experimental results by Dr. Eunkyoung Kim from Dr. Gregory Payne's lab at University of Maryland. Tab. 3 shows the simulation-specific parameters used in the computation of these results.

Table 2: Species-specific Parameters

Parameter	Value
Oxidized Diffusion co-efficient (D_O)	3.79×10^{-6} cm^2/s
Reduced Diffusion co-efficient (D_R)	4.98×10^{-6} cm^2/s
Electrochemical rate constant (k_0)	1.75×10^{-2} cm/s
Charge transfer co-efficient (α)	0.55
Electrons transferred per reaction (n)	1
Temperature (T)	310.15 K

*Ferrocene is in reduced state initially.

Table 3: CV Simulation Parameters

Parameter	Value
Sampling time (Δt)	0.1 s
Sampling space (Δx)	0.0011 cm
Amplitude of voltage signal (v_{amp})	1V
Voltage scan rate (v = $\frac{2v_{amp}}{\tau}$)	0.01 V/s
Electrode surface area (Ar)	0.0314 cm^2

With the parameters stated in the aforementioned three tables, simulations were performed for each frequency of the molecular input concentration signal. The corresponding output of the system for Fc is the negative current peak value. The frequency response of the channel as well as the noise power spectral density were obtained according to the description in Sec. 3.1. Figure 3 displays the **frequency response of the channel** across the range of frequencies stated in Tab. 1. The **noise power spectral density** shown in Fig. 4 was obtained from the electrical output signal across the permutations of frequency and concentration values.

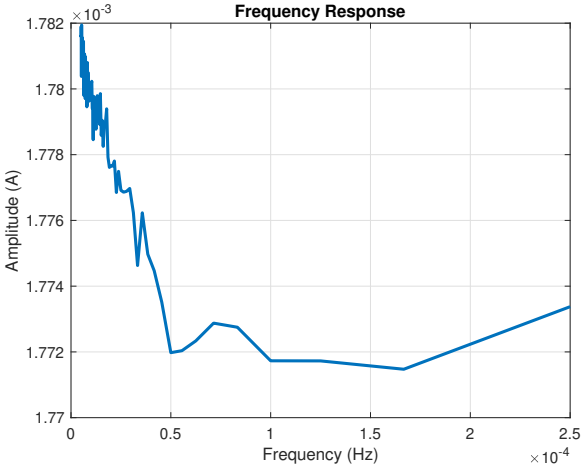

Figure 3: Frequency response of the channel.

The capacity estimation through water filling was implemented with a desired average output signal power of $3.0412\times10^{-7}\ \frac{\mathrm{A^2s^2}}{\mathrm{M^2}}$ (where A stands for Ampere and M stand for Molarity, which is generally measured as moles per liter) as the water line value ν, and by following the steps mentioned in Sec. 3.2. We obtained an initial estimate for the capacity C of $\mathbf{0.0000163}\,\frac{\mathbf{bits}}{\mathbf{sec}}$, which corresponds

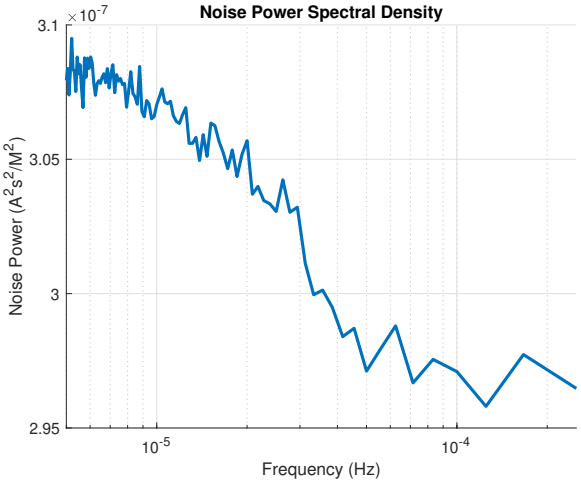

Figure 4: Noise power spectral density with diffusion noise in the channel.

to a value of $\mathbf{0.0587}\frac{\mathbf{bits}}{\mathbf{hour}}$. Given that the time scales of biological processes, especially those envisioned to provide the input to the redox-enabled communication system device described in [6], are of the order of hours or even days, this estimated capacity value is believed to be sufficient for the envisioned applications.

5 CONCLUSION

In this paper, building upon the computational model and the simulation framework for a redox-based molecular-to-electrical communication channel, we introduced an empirical frequency domain analysis. We used an input sinusoidal wave with varying frequencies as the transmitted molecular concentration signal to observe the channel's response as an electrical output current. This analysis enables the characterization of this communication channel from the perspective of the frequency response and the noise power spectral density. From these results, we obtained an initial estimate for the channel capacity using a water filling algorithm, learning that this system could theoretically achieve a capacity of $\mathbf{0.0587}\frac{\mathbf{bits}}{\mathbf{hour}}$, which is in line with the expectations of such an interface. Even if preliminary, these communication theory-based performance metrics in conjunction with system design principles can be used to optimize and engineer redox-based molecular-electrical communications for future MC-enabled systems and devices.

ACKNOWLEDGMENTS

This paper is based upon work supported by the Semiconductor Research Corporation (SRC) through Task No. 2843.001 and the National Science Foundation (NSF) through Grants No. ECCS-1807604 and CCF-1816969. The authors also acknowledge support and experimental setup knowledge from Dr. Gregory F. Payne and Dr. Eunkyoung Kim of Institute for Bioscience and Biotechnology Research (IBBR), University of Maryland.

REFERENCES

[1] Nariman Farsad, H. Birkan Yilmaz, Andrew Eckford, Chan-Byoung Chae, and Weisi Guo. A comprehensive survey of recent advancements in molecular communication. *IEEE Communications Surveys Tutorials*, 18(3):1887–1919, 2016. doi: 10.1109/COMST.2016.2527741.

[2] Ian F. Akyildiz, Massimiliano Pierobon, and Sasitharan Balasubramaniam. Moving Forward with Molecular Communication: From Theory to Human Health Applications, 5 2019. ISSN 15582256.

[3] Ian F. Akyildiz, Massimiliano Pierobon, Sasitharan Balasubramaniam, and Yevgeni Koucheryavy. The internet of Bio-Nano things. *IEEE Communications Magazine*, 53(3):32–40, 3 2015. ISSN 0163-6804. doi: 10.1109/MCOM.2015.7060516. URL http://ieeexplore.ieee.org/document/7060516/.

[4] Nariman Farsad, Weisi Guo, and Andrew W. Eckford. Tabletop molecular communication: Text messages through chemical signals. *PLOS ONE*, 8(12):1–13, 12 2013. doi: 10.1371/journal.pone.0082935. URL https://doi.org/10.1371/journal.pone.0082935.

[5] Xinyi Y. Zhou, Gregory F. Payne, William E. Bentley, Eunkyoung Kim, Hana Ueda, Tanya Tschirhart, and Chen-Yu Tsao. Electrochemical Measurement of the β-Galactosidase Reporter from Live Cells: A Comparison to the Miller Assay. *ACS Synthetic Biology*, 2015. ISSN 2161-5063. doi: 10.1021/acssynbio.5b00073.

[6] Yi Liu, Chen-Yu Tsao, Eunkyoung Kim, Tanya Tschirhart, Jessica L. Terrell, William E. Bentley, and Gregory F. Payne. Using a Redox Modality to Connect Synthetic Biology to Electronics: Hydrogel-Based Chemo-Electro Signal Transduction for Molecular Communication. *Advanced Healthcare Materials*, 6(1):1600908, 1 2017. ISSN 21922640. doi: 10.1002/adhm.201600908. URL http://doi.wiley.com/10.1002/adhm.201600908.

[7] Yi Liu, Jinyang Li, Tanya Tschirhart, Jessica L. Terrell, Eunkyoung Kim, Chen-Yu Tsao, Deanna L. Kelly, William E. Bentley, and Gregory F. Payne. Connecting Biology to Electronics: Molecular Communication via Redox Modality. *Advanced Healthcare Materials*, 6(24):1700789, 12 2017. ISSN 21922640. doi: 10.1002/adhm.201700789. URL http://doi.wiley.com/10.1002/adhm.201700789.

[8] Ian F. Akyildiz, Massimiliano Pierobon, and Sasitharan Balasubramaniam. An Information Theoretic Framework to Analyze Molecular Communication Systems Based on Statistical Mechanics. *Proceedings of the IEEE*, 107(7):1230–1255, 7 2019. ISSN 15582256. doi: 10.1109/JPROC.2019.2927926.

[9] Colton Harper, Massimiliano Pierobon, and Maurizio Magarini. Estimating Information Exchange Performance of Engineered Cell-to-cell Molecular Communications: A Computational Approach. In *IEEE INFOCOM 2018 - IEEE Conference on Computer Communications*, pages 729–737. IEEE, 4 2018. ISBN 978-1-5386-4128-6. doi: 10.1109/INFOCOM.2018.8485834. URL https://ieeexplore.ieee.org/document/8485834/.

[10] Francesca Ratti, Colton Harper, Maurizio Magarini, and Massimiliano Pierobon. Optimizing information transfer through chemical channels in molecular communication. In *2021 IEEE Global Communications Conference (GLOBECOM)*, pages 1–6, 2021. doi: 10.1109/GLOBECOM46510.2021.9685247.

[11] Karthik Reddy Gorla, Tyler Barker, and Massimiliano Pierobon. Modeling Diffusion and Chemical Reactions to Analyze Redox-Based Molecular-Electrical Communication. In *ICC 2020 - 2020 IEEE International Conference on Communications (ICC)*, pages 1–7, 2020. doi: 10.1109/ICC40277.2020.9148750.

[12] Peter J Thomas, Donald J Spencer, Sierra K Hampton, Peter Park, and Joseph P Zurkus. The diffusion-limited biochemical signal-relay channel. In *Advances in Neural Information Processing Systems*, pages 1263–1270. Citeseer, 2004.

[13] Allen J. Bard and Larry R. Faulkner. *Electrochemical methods : fundamentals and applications*. Wiley, 2001. ISBN 9780471043720. URL https://www.wiley.com/en-us/Electrochemical+Methods%3A+Fundamentals+and+Applications%2C+2nd+Edition-p-9780471043720.

[14] Noémie Elgrishi, Kelley J. Rountree, Brian D. McCarthy, Eric S. Rountree, Thomas T. Eisenhart, and Jillian L. Dempsey. A Practical Beginner's Guide to Cyclic Voltammetry. *Journal of Chemical Education*, 95(2):197–206, 2 2018. ISSN 0021-9584. doi: 10.1021/acs.jchemed.7b00361. URL http://pubs.acs.org/doi/10.1021/acs.jchemed.7b00361.

[15] Daniel T. Gillespie. Stochastic simulation of chemical kinetics. *Annual review of physical chemistry*, 58:35–55, 2007. ISSN 0066-426X. doi: 10.1146/ANNUREV.PHYSCHEM.58.032806.104637. URL https://pubmed.ncbi.nlm.nih.gov/17037977/.

[16] Piero Zanello. *Inorganic Electrochemistry*. Royal Society of Chemistry, Cambridge, 8 2007. ISBN 978-0-85404-661-4. doi: 10.1039/9781847551146. URL http://ebook.rsc.org/?DOI=10.1039/9781847551146.

[17] John Proakis. *Digital Communications 5th Edition*. McGraw Hill, 2007.

[18] Peter M. Attia. Cyclic voltammetry simulation tutorials, 209. URL https://petermattia.com/cyclic_voltammetry_simulation/index.html.

[19] Heitor Castro, Robin Bouma, Rustin Haase, Nathan Doher, Tyler Zinsmaster, Beau Ottovy, Karthik Reddy Gorla, and Massimiliano Pierobon. PaRedox: A Software for Parameter-based Design and Optimization of Redox-enabled Bio-electronic Devices, 2021. URL http://paredox.unl.edu.

[20] Robert R. Gagne, Carl A. Koval, and George C. Lisensky. Ferrocene as an Internal Standard for Electrochemical Measurements. *Inorganic Chemistry*, 19(9):2854–2855, 1980. ISSN 1520510X. doi: 10.1021/IC50211A080/ASSET/IC50211A080.FP.PNG{_}V03. URL https://pubs.acs.org/doi/abs/10.1021/ic50211a080.